Design of Bimodal PCL and PCL-HA Nanocomposite Scaffolds by Two Step Depressurization During Solid-state Supercritical CO_2 Foaming

Aurelio Salerno,* Stefania Zeppetelli, Ernesto Di Maio, Salvatore Iannace, Paolo Antonio Netti

This communication reports the design and fabrication of porous scaffolds of poly(ε-caprolactone) (PCL) and PCL loaded with hydroxyapatite (HA) nanoparticles with bimodal pore size distributions by a two step depressurization solid-state supercritical CO_2 ($scCO_2$) foaming process. Results show that the pore structure features of the scaffolds are strongly affected by the thermal history of the starting polymeric materials and by the depressurization profile. In particular, PCL and PCL-HA nanocomposite scaffolds with bimodal and uniform pore size distributions are fabricated by quenching molten samples in liquid N_2, solubilizing the $scCO_2$ at 37 °C and 20 MPa, and further releasing the blowing agent in two steps: (1) from 20 to 10 MPa at a slow depressurization rate, and (2) from 10 MPa to the ambient pressure at a fast depressurization rate. The biocompatibility of the bimodal scaffolds is finally evaluated by the in vitro culture of human mesenchymal stem cells (MSCs), in order to assess their potential for tissue engineering applications.

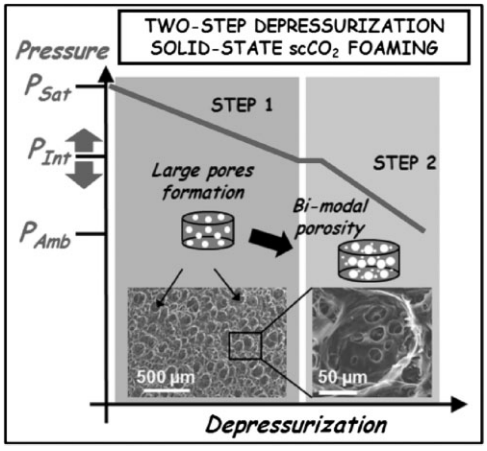

A. Salerno, P. A. Netti
Interdisciplinary Research Centre on Biomaterials (CRIB) and Italian Institute of Technology (IIT), Piazz.le Tecchio 80, 80125 Naples, Italy
E-mail: asalerno@unina.it
A. Salerno, S. Zeppetelli, S. Iannace
Institute of Composite and Biomedical Materials, National Research Council (IMCB-CNR), Piazz.le Tecchio 80, 80125, Naples, Italy
E. Di Maio, P. A. Netti
Department of Materials and Production Engineering, University of Naples Federico II, Piazz.le Tecchio 80, 80125 Naples, Italy

Introduction

Biomaterial scaffolds are key components of tissue engineering (TE) strategies since they have to provide a regenerative cell microenvironment able to mimic the cell-instructive and cell-responsive functions of the extracellular matrix (ECM) in the native biological tissues.[1,2] The scaffold acts as a temporary substitute for the ECM, controlling and guiding cell behavior and new tissue remodelling. To this aim, the scaffold must deliver signalling molecules (e.g., growth factors) in a spatially

© 2011 WILEY-VCH Verlag GmbH & Co. KGaA, Weinheim

DOI: 10.1002/marc.201100119

coordinated and temporally controlled fashion, in order to improve the regenerative potential of transplanted cells.[1,2]

Concerning biomaterials, PCL is one of the most investigated Food and Drug approved biocompatible and biodegradable polymers in TE.[3] Indeed, PCL is characterized by rheological properties that make it easy to be appropriately processed to trigger structural and micro-environmental niches for different cell types, spanning from mesenchymal stem cells (MSCs) to fibroblast and bone cells.[3–5] Furthermore, in the case of bone regeneration, the integration of calcium phosphates particles, such as hydroxyapatite (HA), within PCL scaffolds was reported as an efficient strategy for enhancing their bone regeneration properties.[5b]

Scaffold pore structure plays a key role in TE. In particular, it has been recently demonstrated that a macroporosity of a few hundred microns is necessary to promote three-dimensional adhesion, proliferation and migration of cells, while a microporosity pathway with pore sizes ranging from 1 to 50 microns is necessary for nutrient and metabolic waste transport.[5a,5b,6]

Supercritical CO_2 ($scCO_2$) foaming has achieved great emphasis in TE because it may allow for the fabrication of porous scaffolds and avoids the use of organic solvents that are potentially harmful to cells and tissues.[5b,7,8] Furthermore, the rather low $scCO_2$ temperature (31.1 °C) and pressure (7.4 MPa), in combination with the solvation properties of $scCO_2$, may offer the possibility of simultaneously processing biomaterials, cells and growth factors, aiming to produce bioactive porous scaffolds in a one step process.[7,9] The architecture of the pore structure achievable by this technique may be fine controlled through the proper selection of the processing conditions, mainly solubilization pressure (gas concentration), foaming temperature and pressure drop rate.[5a,5b,10,11] Furthermore, by a two step depressurization foaming, it has been also possible to design polymeric foams with a bimodal distribution of pore sizes.[12,13] However, to date, this approach has mainly been applied to amorphous polymers, such as polystyrene, while there are a lack of investigations focusing on semi-crystalline and biocompatible polymers like PCL.

Semi-crystalline polymers may be considered as two phase systems in which the crystallites are dispersed in the amorphous matrix. The crystallites nucleate and grow from the melt as well as from the rubbery phase and, depending on the processing parameters and the presence of suitable additives within the polymeric matrix, they aggregate to form spherulites of different morphology, size and structure.[14] Solid-state $scCO_2$ foaming is relatively simple to apply to completely amorphous polymers, like polystyrene, because of the capability of the blowing agent to easily diffuse within the amorphous, glassy phase and "plasticize" the polymer to render it rubbery.[14] In contrast, the solid-state foaming of semi-crystalline polymers, like PCL, is more difficult owing to the different $scCO_2$ solubility and diffusivity within the amorphous and crystalline domains and due to the presence of non-plasticized crystal regions maintaining a high viscosity/stiffness and therefore hindering, when possible, uniform pore nucleation and growth.[14–16]

This work reports for the first time the two step depressurization solid-state $scCO_2$ foaming of PCL and PCL-HA nanocomposite, with the aim of designing bimodal porous scaffolds for TE. The so-called "solid-state" means that the solubilization and foaming temperatures were chosen to be well below the melting temperature of PCL and, in particular, fixed at 37 °C, in order to open up the possibility of further incorporation of cells and bioactive moieties within the scaffolds during the fabrication process.[7,9]

Experimental Section

Materials and Methods

PCL ($\overline{M}_w = 65$ kDa, $T_m = 59$–64 °C, Sigma-Aldrich, Italy) and 5 wt% of HA nanoparticles (100 nm mean size, Berkeley Advanced Biomaterials Inc., Berkeley, CA) were melt mixed using an internal mixer (Rheomix® 600-Rheocord® 9000, Haake, Germany). The as-obtained nanocomposite was compression moulded at 80 °C using a hot press (P 300 P, Collin, Germany) to prepare 200 μm thick films, and further subjected to two different non-isothermal cooling processes: in one process, the melted samples were slowly cooled from 80 to 25 °C (15 min, approximately), while for the other cooling process, the melted samples were quickly cooled by immersing in liquid N_2. Neat PCL was subjected to the same processes for proper comparison.

Samples for $scCO_2$ foaming experiments were obtained by overlapping five disc-shaped samples ($d = 10$ mm, thickness = 200 μm) characterized by the same composition and thermal history. The samples were placed in a high pressure vessel (HiP, Pennsylvania, USA), previously cooled to 5 °C, and the CO_2 was subsequently introduced into the vessel up to a pressure of 5 MPa. The temperature and pressure of the vessel were further increased to 37 °C and 20 MPa, respectively, and $scCO_2$ solubilization was carried out for 1.5 h. Foaming experiments were carried out by solubilizing the samples at a saturation pressure of 20 MPa for 1.5 h. Subsequently, the pressure was slowly released to an intermediate pressure, in the range from 6 to 10 MPa, by a first non-isothermal depressurization step, in order to promote the nucleation and growth of large pores.[11] The time of depressurization was varied from 1 to 10 min, depending on the intermediate pressure. The temperature of the system was then allowed to re-equilibrate at 37 °C, and, after 5 min, the pressure was finally released to ambient in 1–2 s, to promote the formation of tiny pores, to achieve a bimodal distribution of pore sizes.

The thermal properties of PCL and PCL-HA nanocomposite were assessed by thermo-gravimetric (TGA/DTGA) and differential scanning calorimetric (DSC) analyses. For the TGA/DTGA test, the samples were analyzed from 30 to 650 °C at 10 °C min^{-1} under

© 2011 WILEY-VCH Verlag GmbH & Co. KGaA, Weinheim

an inert atmosphere using a TGA 2950 (TA Instruments, USA). For DSC analysis (DSC Q1000, TA Instruments, USA), 10 mg samples were scanned from 10 to 80 °C at 2 °C min^{-1} under an inert atmosphere. The DSC tests were also performed on the samples after the $scCO_2$ treatment at 37 °C and 20 MPa for 1.5 h in order to assess the effect of the effect of the $scCO_2$ sorption/desorption on the thermal properties of the samples. When opening the vessel, to minimize polymer foaming during depressurization, the samples were cooled down to 5 °C and the pressure was slowly decreased to ambient (2 h approximately).

TEM and SEM microscopy analyses were used to evaluate the morphology and distribution of the HA nanoparticles within the polymeric matrix, and to assess the morphology of the scaffolds, respectively. Samples for TEM analysis were prepared by sectioning 100 nm thick slices of the PCL-HA nanocomposite with a LKB ultramicrotome, and analyzed at an acceleration voltage of 100 kV with a Philips EM 208 (Eindhoven, The Netherlands). For SEM tests, the scaffolds were cross-sectioned with a razor blade, gold sputtered and analyzed by SEM (S440, LEICA, Germany).

The porosity, pore size distribution and pore density (N_f) of the scaffolds were determined by gravimetric measurements and image analysis, as described in previously reported works.[5a,13]

The biocompatibility of the scaffolds was assessed by using bone marrow-derived human MSCs (Clonetics). The scaffolds ($d = 10$ mm and $h = 4$ mm) were γ-sterilized at 2.5 Mrad for 8 min and statically seeded with 6.4 cell cm^{-2}, and re-suspended in 50 mL of medium. The cell/scaffold constructs were subsequently placed in 24 well culture plates (1 scaffold/well). After 24 h of incubation in α-Modified Eagle's medium (α-MEM) (Bio Wittaker, Belgium), cell adhesion and morphology were assessed by confocal laser scanning microscope (CLSM) analysis. The constructs were fixed with 4% paraformaldehyde for 20 min at RT, rinsed twice with PBS buffer, and incubated with PBS-BSA 0.5% to block unspecific binding. Actin microfilaments were stained with phalloidin tetramethylrhodamine B isothiocyanate (Sigma-Aldrich) diluted in PBS-BSA 0.5% for 30 min at RT. The constructs were then rinsed three times with PBS and observed by CLSM (LSM510; Zeiss).

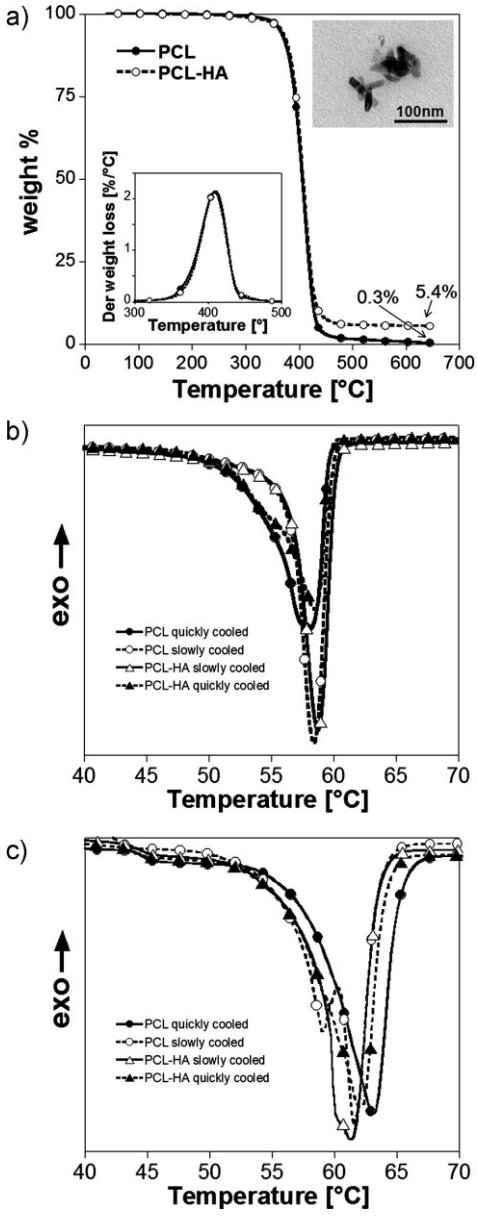

Figure 1. (a) TGA/DTGA results for neat PCL and PCL-HA nanocomposite; DSC 1st heating scan (2 °C min^{-1}) of PCL and PCL-HA nanocomposite prepared by the slow and quick non-isothermal cooling processes before (b) and after (c) the $scCO_2$ treatment.

Results and Discussion

Before foaming, the materials were characterized in order to assess the morphology and distribution of the HA nanoparticles within the polymeric matrix and to evaluate the effect of the composition, cooling process and $scCO_2$ treatment on their thermal properties.

As shown in the TEM micrograph reported in the inset of Figure 1(a), commercially available rod-like HA nanoparticles, characterized by a length of 100 nm, were dispersed within PCL to improve its bone regeneration potential.[5a,5b] The TGA/DTGA results in Figure 1(a) show that the HA produced a residue at 650 °C close to its nominal amount, equal to 5 wt%, while it did not induce significant changes in the thermal degradation of the polymer, which occurred in the 300–500 °C temperature range.[5a]

The DSC results reported in Figure 1(b) and 1(c) showed the melting peak of the samples before and after the $scCO_2$ treatment, respectively. The melting peak and the crystalline fraction of PCL slightly decreased from 58.5 °C and 66.7% for the slowly cooled PCL film, to 58.1 °C and 65.9%, respectively, when the PCL was cooled in liquid N_2. Furthermore, as shown in Figure 1(b), the PCL film quenched in liquid N_2 was characterized by a 2 °C decrease in its initial melting temperature, and by the presence of marked endothermic shoulders near 50 °C. Similar results were achieved for the PCL-HA nanocomposite, indicating that the "instantaneous" cooling in liquid N_2 induced the formation of a more heterogeneous population of spherulites

© 2011 WILEY-VCH Verlag GmbH & Co. KGaA, Weinheim

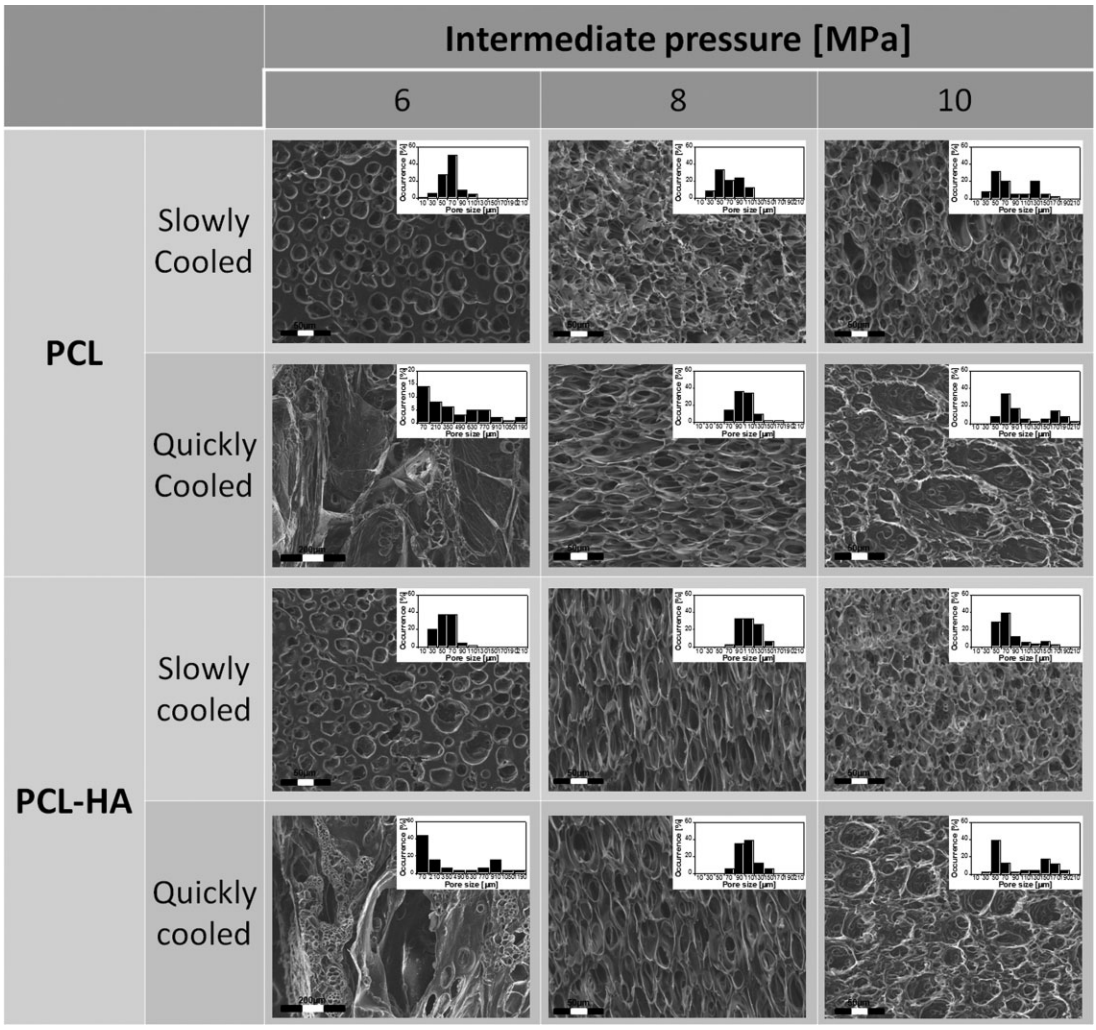

Figure 2. Morphology and pore size distribution of the PCL and PCL-HA nanocomposite scaffolds as a function of the intermediate pressure and thermal history.

characterized by reduced thermal stability and, therefore, melting at lower temperatures.[14] The melting properties of the samples significantly changed after the $scCO_2$ treatment. Indeed, all of the $scCO_2$-crystallized samples evidenced higher melting peak values and crystallinity when compared to the untreated ones. It is important to point out that this effect was more marked for the PCL and PCL-HA samples quenched in liquid N_2, for which the melting peak increased to 64 and 63 °C, respectively. These results indicated that the solid-state $scCO_2$ melting of the materials was promoted by the increase of their cooling rate. As a direct consequence, relevant changes in the structure of the materials were induced when treated with the $scCO_2$, even if the treatment did not cancel their thermal histories, as demonstrated by the differences among the materials evidenced in Figure 1(c).

The optimization of the pore structure of PCL and PCL-HA nanocomposite scaffolds was obtained by performing a systematic investigation on the effect of the formulation of the samples and their thermal history on the morphology, porosity and pore size distribution of foams achievable by a two step depressurization solid-state $scCO_2$ foaming.

The results on the morphology and pore size distribution of the scaffolds are shown in Figure 2. The depressurization profile had a strong impact on the pore structure features of the scaffolds. In particular, at the intermediate pressure of 10 MPa, we obtained porous PCL and PCL-HA scaffolds with bimodal pore size distributions that were characterized by a macro-porosity, with pore sizes in the range 100 to 300 μm, and a micro-porosity with a mean pore size in the 50–70 μm range. Furthermore, for these samples, an increase in the cooling rate resulted in a slight increase in the size and extent of the macro-porosity. When the intermediate pressure decreased down to 8 MPa, the scaffolds showed a mono-modal pore size distribution and a high degree of pores interconnection. Interestingly, depending on the

© 2011 WILEY-VCH Verlag GmbH & Co. KGaA, Weinheim

thermal history of the PCL and PCL-HA films, completely different pore structure features were observed at the intermediate pressure of 6 MPa. In effect, when prepared from slowly cooled films, the PCL and PCL-HA scaffolds evidenced mono-modal pore size distributions with mean pore sizes equal to 65 ± 18 μm and 57 ± 21 μm, respectively. Conversely, the samples quenched in liquid N_2 produced porous scaffolds with a bimodal distribution of pores size and non-homogeneous morphologies. In particular, smaller pores with a mean size equal to 93 ± 28 μm for neat PCL and to 65 ± 31 μm for PCL-HA, were randomly distributed all around very large pores, characterized by mean pore sizes equal to 614 ± 269 μm and 745 ± 345 μm, respectively.

Figure 3 reports the effect of the intermediate pressure on the porosity and pore density of the scaffolds. As shown, the porosity was dependent on both the thermal properties and the pressure drop profile. In particular, we observed a decrease in the porosity of the scaffolds with an increase in the intermediate pressure from 7 to 10 MPa. Furthermore, the samples quenched in liquid N_2 were characterized by higher porosity values over the whole range of intermediate pressures investigated. This difference was particularly evident at the intermediate pressure of 6 MPa, for which the porosity of the PCL and PCL-HA scaffolds increased from 59.1 and 58.8% for the slowly cooled samples, to 93.2 and 89.3%, respectively, for the non-isothermal cooling performed in liquid N_2. All of the samples evidenced an increase in the pore density when the intermediate pressure increased from 6 to 10 MPa, followed by a decrease when the intermediate pressure further increased to 10 MPa. In agreement with the morphological results in Figure 2, at the intermediate pressure of 6 MPa, a two order of magnitude higher pore density was observed in the case of the quickly cooled PCL and PCL-HA samples when compared to the slowly cooled ones. All of these results clearly demonstrate that control of the pore structure features of porous PCL and PCL-HA nanocomposite scaffolds prepared by solid-state $scCO_2$ foaming strongly depends on control of the thermal history of the polymers, as well as the depressurization profile.

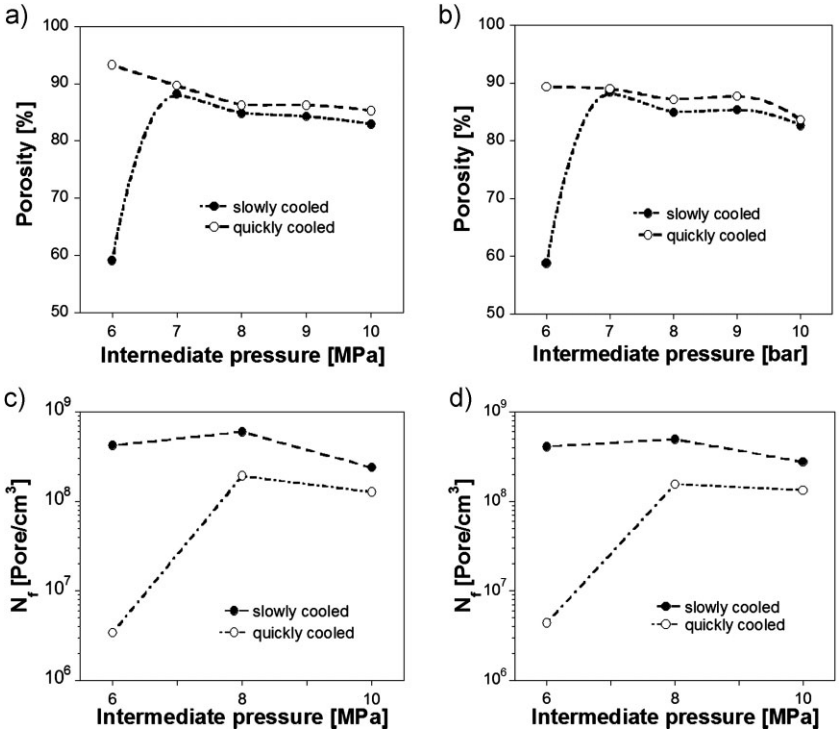

Figure 3. Porosity (a and b) and pore density (c and d) of the (a,c) PCL and (b,d) PCL-HA nanocomposite scaffolds as a function of the intermediate pressure and thermal history.

Few studies have been reported about the solid-state $scCO_2$ foaming of PCL,[10,16] whereas several investigations have been performed on the $scCO_2$ foaming of PCL at temperatures above its melting temperature.[11,17,18] Making this process suitable for the incorporation of heat labile molecules within the scaffold before the foaming process may represent a great challenge in TE;[7,9] in this work we focused on the solid-state foaming of PCL and PCL-HA nanocomposite and performed the entire process at 37 °C.

The results of our study indicate that both thermal history and pressure drop profile have a key role in the final scaffold's pore structure. Doroudiani et al. investigated the effect of the thermal history on the solid-state foaming of semi-crystalline polymers, like polyethylene and polypropylene.[14] In agreement with our results, in their study the authors reported that the extent of foaming increased with increasing cooling rate, as a consequence of the enhanced fraction of amorphous phase within the polymers that resulted in improved $scCO_2$ solubilization and foaming, as previously discussed. Although our results evidenced minor differences between the crystalline fraction of the PCL and PCL-HA samples as a function of the thermal history, the DSC results in Figure 1(b) suggest that the samples quenched in liquid N_2 started to melt at lower temperatures and, therefore, probably enhance the plasticizing effect of $scCO_2$. This consideration is supported by the DSC results in Figure 1(c) and is also corroborated by literature data showing that, when in contact with $scCO_2$, PCL may undergo a partial or complete melting at a temperature well below its melting point.[19–21] In particular, Shieh et al.

© 2011 WILEY-VCH Verlag GmbH & Co. KGaA, Weinheim

investigated the effect of the pressure of $scCO_2$ on PCL melting, reporting that the extent of melting increased with increasing the pressure from 3.6 to 30 MPa.[19] Accordingly, Lian et al. showed that the solubilization of the $scCO_2$ at a pressure of 10 MPa induced melting point depression of PCL to 37 °C.[20] These results were also supported by those reported by Kiran et al. who demonstrated that PCL melted at 35 °C for a $scCO_2$ pressure of 21 MPa, and further re-crystallized during the $scCO_2$ desorption step.[21] By considering the processing conditions used in this study, completely different CO_2 solubilization and polymer plasticization may be expected as a function of the thermal history of the samples and, in turn, PCL and PCL-HA scaffolds with higher porosities (Figure 3) and larger pores size (Figure 2) were obtained starting from the films quenched in liquid N_2. However, further investigations will be necessary to evaluate the effect of the cooling processes on the crystalline structure of PCL and PCL-HA nanocomposite and, therefore, on the $scCO_2$ solubilization and foaming. The peculiar behavior observed at the intermediate pressure of 6 MPa as a function of the thermal history of the samples is ascribable to the fact that, during the first step of depressurization, the $scCO_2$ undergoes a change from a supercritical to a gaseous state. This effect, together with the long time (up to 15 min) required to drop the pressure from 20 to 6 MPa, induced the growth and nucleation of very large pores within the samples cooled in liquid N_2. The further reduction of the pressure from 6 to 0.1 MPa during the second depressurization step allowed for the nucleation of smaller pores within the unfoamed polymer (Figure 3) and the further growth of the large pores.[12,13] As previously discussed, the different solubility and the reduced plasticization power of the blowing agent within the slowly cooled samples (Figure 1) induced the formation of inhomogeneous polymer-CO_2 systems characterized by unplasticized crystalline regions that increased the stiffness of the samples and decreased their foaming. This effect was mainly evident at higher depressurization times and, therefore, in the case of the intermediate pressure of 6 MPa, even if these samples produced scaffolds with more homogeneous morphologies.

Taking into the account all of these results, in this study we carried out a preliminary biological investigation on the PCL scaffolds obtained, starting from the samples quenched in liquid N_2 and selecting an intermediate pressure of 10 MPa. The tests have been performed in vitro by statically seeding human MSCs onto the surface of the scaffolds. Figure 4 reports CLSM images of (a) the control (scaffold w/o cells) and (b) the cell/scaffold construct after 24 h of in vitro culture. As shown, the cells uniformly colonized the seeding surface of the PCL scaffold, adhering to the pore walls and creating cell-to-cell communications (white arrows).

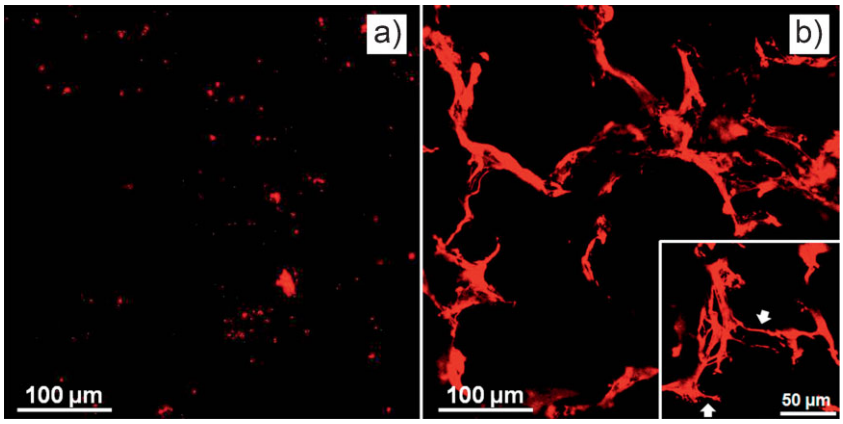

Figure 4. (a) CLSM image of a bimodal PCL scaffold without cells after 24 h of incubation in vitro; (b) CLSM image of the hMSCs seeded onto the bimodal PCL scaffold after 24 h of incubation in vitro.

Conclusion

In this study we investigated the two step depressurization solid-state $scCO_2$ foaming of PCL and PCL-HA nanocomposite, aiming to design porous three-dimensional scaffolds for TE.

The results demonstrated that control of the thermal history and intermediate pressure is essential to design scaffolds with homogeneous and bimodal pore size distributions. In conclusion, the novel results reported in this work may open up new routes for the design of porous bioactive PCL and PCL-HA nanocomposite scaffolds with improved TE performance.

Acknowledgements: This research has been supported by a grant from the Italian Ministry of Health, TISSUENET n. RBPR05RSM2.

Received: March 1, 2011; Revised: May 6, 2011; Published online: June 3, 2011; DOI: 10.1002/marc.201100119

Keywords: foams; nanocomposites; poly(ε-caprolactone); structure; supports

[1] M. P. Lutolf, J. A. Hubbell, *Advances in Tissue Engineering: Synthetic biomaterials as cell-responsive artificial extracellular matrices*, Imperial College Press, London **2008**.
[2] S. Huang, X. Fu, *J. Controlled Release* **2010**, *142*, 149.
[3] M. A. Woodruff, D. W. Hutmacher, *Progr. Polym. Sci.* **2010**, *35*, 1217.

© 2011 WILEY-VCH Verlag GmbH & Co. KGaA, Weinheim

[4] S. H. Oh, I. K. Park, J. M. Kim, J. H. Lee, *Biomaterials.* **2007**, *28*, 1664.
[5] [5a] A. Salerno, S. Zeppetelli, E. Di Maio, S. Iannace, P. A. Netti, *Biotech. Bioeng.* **2010**, *108*, 963; [5b] A. Salerno, S. Zeppetelli, E. Di Maio, S. Iannace, P. A. Netti, *Comp. Sci. Tech.* **2010**, *70*, 1838.
[6] M. M. C. G. Silva, L. A. Cyster, J- J. A. Barry, X. B. Yang, R. O. C. Oreffo, D. M. Grant, C. A. Scotchford, S. M. Howdle, K. M. Shakesheff, F. R. A. J. Rose, *Biomaterials* **2006**, *27*, 5909.
[7] D. D. Hile, M. L. Amirpour, A. Akgerman, M. V. Pishko, *J. Controlled Release* **2000**, *66*, 177.
[8] X. H. Zhu, L. Y. Lee, J. S. H. Jackson, Y. W. Tong, C. Wang, *Biotech. Bioeng.* **2008**, *100*, 998.
[9] P. J. Ginty, D. Howard, C. E. Upton, J. J. A. Barry, F. R. A. J. Rose, K. M. Shakesheff, S. M. Howdle, *J. Super. Fluids* **2008**, *43*, 535.
[10] A. Léonard, C. Calberg, G. Kerckhofs, M. Wevers, R. Jeérôme, J. Pirard, A. Germain, S. Blacher, *J. Porous Mater.* **2008**, *15*, 397.
[11] C. Gualandi, L. J. White, L. Chen, R. A. Gross, K. M. Shakesheff, S. M. Howdle, M. Scandola, *Acta Biomater.* **2010**, *6*, 130.
[12] K. A. Arora, A. J. Lesser, T. J. McCarthy, *Macromolecules.* **1998**, *31*, 4614.
[13] J. Bao, T. Liu, L. Zhao, G. Hu, *J. Super. Fluids* **2010**, DOI: 10.1016/j.supflu.2010.09.032.
[14] S. Doroudiani, C. B. Park, M. T. Kortschot, *Polym. Eng. Sci.* **1996**, *36*, 2645.
[15] X. Jiang, T. Liu, Z. Xu, L. Zhao, G. Hub, W. Yuan, *J. Super. Fluids* **2009**, *48*, 167.
[16] Q. Xu, X. Ren, Y. Chang, J. Wang, L. Yu, K. Dean, *J. Appl. Polym. Sci.* **2004**, *94*, 593.
[17] J. Reignier, R. Gendron, M. F. Champagne, *J. Cell. Plastics* **2007**, *43*, 459.
[18] K. Luetzow, F. Klein, T. Weigel, R. Apostel, A. Weiss, A. Lendlein, *J. Biomech.* **2007**, *40*, S80.
[19] Y. Shieh, H. Yang, *J. Super. Fluids* **2005**, *33*, 183.
[20] Z. Lian, S. A. Epstein, C. W. Blenk, A. D. Shine, *J. Super. Fluids* **2006**, *39*, 107.
[21] E. Kiran, K. Liu, K. Ramsdell, *Polymer.* **2008**, *49*, 1853.

© 2011 WILEY-VCH Verlag GmbH & Co. KGaA, Weinheim